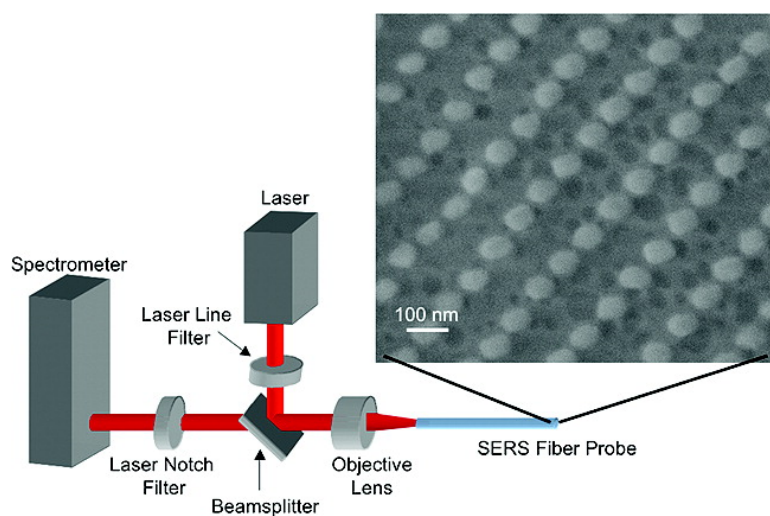


Optical Antenna Arrays on a Fiber Facet for *in Situ* Surface-Enhanced Raman Scattering Detection

Elizabeth J. Smythe, Michael D. Dickey, Jiming Bao, George M. Whitesides, and Federico Capasso

Nano Lett., 2009, 9 (3), 1132-1138 • DOI: 10.1021/nl803668u • Publication Date (Web): 23 February 2009

Downloaded from <http://pubs.acs.org> on March 13, 2009



More About This Article

Additional resources and features associated with this article are available within the HTML version:

- Supporting Information
- Access to high resolution figures
- Links to articles and content related to this article
- Copyright permission to reproduce figures and/or text from this article

[View the Full Text HTML](#)



ACS Publications
High quality. High impact.

Optical Antenna Arrays on a Fiber Facet for *in Situ* Surface-Enhanced Raman Scattering Detection

Elizabeth J. Smythe,[†] Michael D. Dickey,[‡] Jiming Bao,[†] George M. Whitesides,[‡] and Federico Capasso^{*,†}

School of Engineering and Applied Sciences, Harvard University, 29 Oxford Street, Cambridge, Massachusetts 02138, and Department of Chemistry and Chemical Biology, Harvard University, 12 Oxford Street, Cambridge, Massachusetts 02138

Received December 4, 2008; Revised Manuscript Received February 10, 2009

ABSTRACT

This paper reports a bidirectional fiber optic probe for the detection of surface-enhanced Raman scattering (SERS). One facet of the probe features an array of gold optical antennas designed to enhance Raman signals, while the other facet of the fiber is used for the input and collection of light. Simultaneous detection of benzenethiol and 2-[(*E*)-2-pyridin-4-ylethenyl]pyridine is demonstrated through a 35 cm long fiber. The array of nanoscale optical antennas was first defined by electron-beam lithography on a silicon wafer. The array was subsequently stripped from the wafer and then transferred to the facet of a fiber. Lithographic definition of the antennas provides a method for producing two-dimensional arrays with well-defined geometry, which allows (i) the optical response of the probe to be tuned and (ii) the density of “hot spots” generating the enhanced Raman signal to be controlled. It is difficult to determine the Raman signal enhancement factor (EF) of most fiber optic Raman sensors featuring hot spots because the geometry of the Raman enhancing nanostructures is poorly defined. The ability to control the size and spacing of the antennas enables the EF of the transferred array to be estimated. EF values estimated after focusing a laser directly onto the transferred array ranged from 2.6×10^5 to 5.1×10^5 .

This Letter describes the incorporation of an array of gold optical antennas onto the facet of an optical fiber and demonstrates the utility of this device as a probe for *in situ* surface-enhanced Raman scattering (SERS) detection. The coupled antennas function as an ensemble whose surface plasmons resonate with the incident light; these antennas ultimately enhance the weak Raman signal generated by analytes near their surface. The other facet is used to couple excitation light into the probe and detect the enhanced Raman signal that returns through the fiber. The flexibility, durability, and large aspect ratio (length-to-diameter) of optical fibers make them well-suited for remote SERS detection. The optical antennas proved to be an essential element of the probe: the Raman signal from analytes was undetectable through bare, unmodified fibers. We fabricated the gold antennas on a silicon wafer with electron-beam lithography and lift-off, stripped them from the substrate using a thin sacrificial thiol-ene film, and then transferred them to a silica facet.¹ The integration of a lithographically defined SERS array distinguishes this device from previously reported fiber optic probes. Lithography provides control of the geometry of the array and thereby enables the optical response of a

probe to be optimized for a combination of excitation wavelengths and analyte SERS signal. In addition, the use of a uniform and repeating pattern of Raman enhancing sites—which is made possible by using lithography to define the array—enables the calculation of the SERS enhancement factor (EF) of the transferred optical antennas array.

Background. Detection of Raman scattering with an optical fiber is a topic that has generated much interest because it offers the ability to probe solutions *in situ*. Raman scattering is useful for detecting and identifying different chemicals and occurs because molecules interacting with light vibrate and produce inelastically scattered photons with spectra uniquely determined by the composition and structure of the molecule. In general, Raman scattering is weak: SERS utilizes surface plasmons to enhance the Raman signal many orders of magnitude.² Thin, flexible optical fibers are an ideal platform for detecting the SERS signal generated by analytes in remote and/or small samples. Without the presence of a SERS surface, however, a facet of an optical fiber cannot typically collect a detectable amount of Raman signal from a sample. We sought to incorporate a SERS surface with a large signal enhancement onto the facet of an optical fiber such that the signal would be easily detectable.

SERS occurs at points on a metal/dielectric interface where surface plasmons (coherent oscillations of electrons)

[†] School of Engineering and Applied Sciences.

[‡] Department of Chemistry and Chemical Biology.

are generated by incident light. At these points the magnitudes of both the incident electric field and the electric field of the Stokes-shifted Raman scattering signal of nearby analytes are enhanced. Various types of surfaces have been used as SERS substrates. One commonly used SERS substrate is a roughened surface coated with metal:^{3,4} this surface produces sharp points that can provide localized enhancements of a Raman signal.^{5,6} These sharp points are effective at generating a SERS signal and are randomly distributed across the substrate with various shapes and spacing. An arbitrary pattern of metallic nanoparticles, however, is generally not the optimal sample configuration for maximizing the SERS signal measured in a detector: the strength and directionality of enhanced electric fields radiated by a particle are highly dependent on the size and shape of the nanoparticle. Nonoptimal coupling of light to nanoparticles can result in the excitation of lossy, nonradiative surface plasmon modes as well as inefficient scattering of the SERS signal.

Lithographic techniques enable the definition of SERS substrates with nanostructures of specific shapes and spacing. Different nanostructure configurations have been examined, and many studies have analyzed the properties of arrays of metallic optical antennas. The geometry of an individual antenna can be designed to allow the conduction electrons to oscillate resonantly when illuminated with particular frequencies of light. These resonant oscillations of electrons are known as localized surface plasmon resonances (LSPR) and can result in a surface-charge distribution across the antenna that is similar to an oscillating electric dipole. Resonance occurs over a range of frequencies defined by the geometry of the antenna. When the LSPR is excited, large field intensities can form near the tips of the optical antenna. When two of these antennas are placed near one another and illuminated (assuming the antennas are aligned along their long axes), they can act as a pair of coupled dipoles. The electric field enhancement in the gap between the optical antennas often increases relative to the single dipole case, and results in a “hot spot” of stronger Raman signal enhancement.⁷ The resonance of a periodic array of antennas can be tuned by varying the size and spacing of the antennas.^{8–12} We sought to incorporate arrays of coupled optical antennas, designed to resonate with the incident light and the Raman signal of analytes, onto the facet of an optical fiber.

There are a number of SERS probes that collect signal through a fiber, but they are illuminated externally (i.e., unidirectional light propagation).^{13–17} In these schemes, light interacts with the analyte and SERS surface (located on or near a probe facet), and a portion of the generated Raman signal is collected in the fiber and measured at the opposite end. In many situations (e.g., *in situ* detection), external illumination is either undesirable or not feasible; instead, optical fibers can be used to both deliver the irradiating light and collect the resulting SERS signal. This capability is made possible by bidirectional propagation of the excitation light.

Bidirectional probes have been implemented with both a hollow core photonic crystal fiber (HCPCF; ≤ 20 cm in length) and optical communications fiber (≤ 8 cm in length).^{18–23} In most HCPCF devices, the SERS surface is not directly attached to the fiber. Instead, silver nanoparticles mixed with the solution of analyte enhance the Raman signal, which is collected by the HCPCF.^{18–20} However, in many cases, it is undesirable or impractical to add nanoparticles to the solution of analyte. Alternatively, SERS surfaces have been incorporated directly on the facet of silica fiber. These probes consist of a fiber with a modified facet (e.g., the silica is roughened^{21,22} or the facet is covered with an array of self-assembled colloids²³) coated with a thin layer of metal. Although the roughened SERS surfaces enhance the Raman signal of nearby analytes, they have a distribution of feature shapes and sizes that produce the enhanced signal: the location and number of these areas are hard to control and vary among probes. Probes with colloidal self-assemblies have improved periodicity of the SERS hot spots, but their density is still somewhat unpredictable due to packing defects occurring in the colloidal assembly. Their spatial arrangement is also limited to the hexagonal close packed structure assumed by the colloidal assembly.²⁴ The wavelength response of these various SERS fiber-probe surfaces cannot be easily controlled, and the unknown number and location of hot spots on these fiber-probe surfaces prevents calculation of their “enhancement factor” (EF), the standard figure of merit used to compare SERS surfaces.

Optical fiber probes for detecting Raman signals from remote analytes are commercially available (Renishaw, Thermo Scientific, InPhotonics); however most of these probes collect the Raman signal scattered by the sample rather than that generated by SERS. Additionally, these probes are usually housed in rigid, large (~ 10 mm diameter) casings to provide room for alignment of the optics needed to focus light onto the sample and collect the Raman signal. We chose to create a thin, flexible single-fiber SERS probe for the remote detection of small samples; analysis of such samples would prove challenging for most commercially available probes.

Probe Fabrication. We sought to fabricate a periodic array of sub-100-nm gold nanostructures onto the facet of a fiber. We found that using focused-ion-beam milling to define gold nanostructures directly on the facet of the fiber resulted in inadvertent doping of the silica and gold with gallium ions; these ions altered the optical response of the array.²⁵ Electron-beam lithography can define high-resolution patterns of nearly arbitrary features, but it is difficult to apply this technique to the facet of an optical fiber. We therefore used a “decals transfer” technique that allows lithographically defined features to be transferred to the facet of an optical fiber.¹ Briefly, we patterned the SERS surface (a periodic array of gold optical antennas) on a silicon substrate using standard fabrication techniques: electron-beam (e-beam) lithography, e-beam evaporation, and lift-off. We stripped the array off the silicon using a thin (~ 200 nm) film of polymer (thiol-ene). The thin film had a backing of poly(dimethylsiloxane) (PDMS) to provide mechanical support.

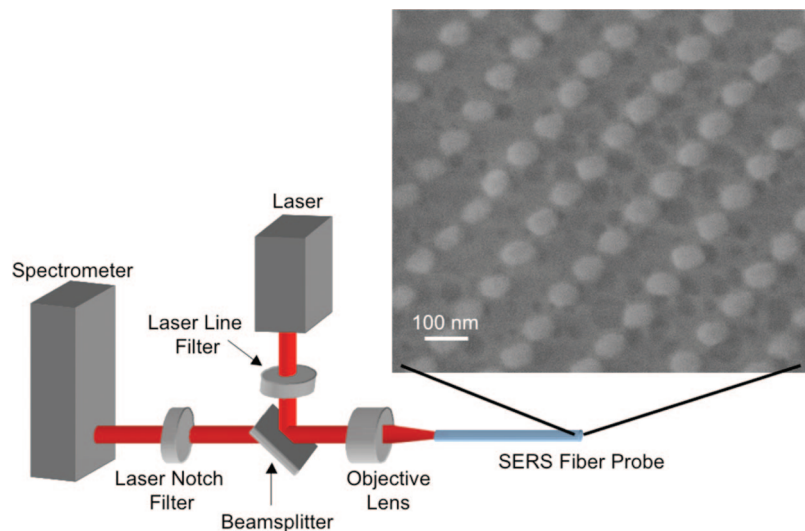


Figure 1. Schematic depiction of the configuration used to characterize the SERS fiber optic probe and a scanning electron micrograph of an array of gold optical antennas on the facet of a fiber. The lithographically defined array allows the SERS signal of nearby analytes to be detected. Laser light coupled into the fiber probe excites the surface plasmon resonance of the array, creating localized hot spots of enhanced electric fields between the coupled antennas. Molecules interacting with these strong fields produce an inelastically scattered Stokes Raman signal; this signal is itself enhanced by the strong electric fields generated by the SERS surface. The Raman signal coupled back into the fiber is detected by the spectrometer.

Pressing the facet of a fiber onto the film caused it (along with the attached antennas) to release from the PDMS and transfer to the fiber. An oxygen plasma etched away the sacrificial thiol-ene film, leaving the array of gold antennas flush with the facet of the fiber. We did not use an adhesion layer between the optical antennas and the glass fiber; we believe that van der Waals forces hold the gold particles to the facet of the fiber.

We designed the coupled antenna array to have a SPR that peaked at a wavelength of ~ 650 nm and spanned wavelengths of ~ 600 – 725 nm. This resonance is broad enough to provide enhancement for both the excitation light ($\lambda = 632.8$ nm) and the Raman signal of the analytes, which ranges between $\lambda \approx 675$ nm and $\lambda \approx 706$ nm. The geometry of the array could be altered to tune the SPR and allow the probes to resonate with different excitation wavelengths.^{12,26,27}

We tested 35 cm long probes made from standard silica fiber (ThorLabs GIF625, NA = 0.275). We transferred an array of coupled optical antennas to one facet of the fiber and cleaved the other to expose a smooth silica surface. The array consisted of gold antennas ~ 65 nm long, 50 nm wide, and 40 nm tall, separated by gaps of 25 nm along their long axis and 100 nm along their short axis. The array spanned a $100 \mu\text{m} \times 100 \mu\text{m}$ area, and completely covered the core of the fiber ($62.5 \mu\text{m}$ in diameter). The scanning electron micrograph in Figure 1 shows a portion of the facet of the fiber optic probe with the transferred array of antennas. The textured background is generated during the oxygen plasma removal of the thiol-ene film and is found on areas of the facet both with and without the array; the presence of this fabrication artifact had no observable effects during the SERS measurements.

SERS Measurements. Before taking Raman measurements, we determined the SPR spectral response of an array on the facet of a fiber by focusing a polarized broadband

white light source directly onto the array, recording the reflected spectrum, and then normalizing it by the reflection of the polarized white light from a silver mirror. The arrays exhibited a strong, broad SPR centered at wavelength of 650 nm when irradiated with incident light polarized along the long axis of the optical antennas. The SPR spanned $\lambda = 600$ nm to $\lambda = 725$ nm and proved broad enough to be excited by the input light ($\lambda = 632.8$ nm) and also to enhance the Raman signal of both benzenethiol and 4-[(*E*)-2-pyridin-4-ylethenyl]pyridine. We did not detect any SPR with the white light polarized perpendicular to the long axis of the antennas. The SPR spectra measured from transferred arrays are shown in the Supporting Information.

We prepared the probe for SERS measurements by immersing the end of the fiber featuring the array in a 3 mM benzenethiol solution (Sigma Aldrich) in methanol. After 12 h we removed the modified facet of the fiber, rinsed it in methanol (removing any benzenethiol molecules not absorbed to the gold antennas), and gently dried it with nitrogen. As shown schematically in Figure 1, we focused the excitation light (helium–neon laser, $\lambda = 632.8$ nm, 5.4 mW) with a $20\times$ objective lens (Mitutoyo, NA = 0.42, working distance = 20 mm) onto the smooth, nonmodified facet of the fiber. We used a laser line filter to remove the secondary emission lines of the laser (ThorLabs, center wavelength = 632.8 ± 2 nm). After propagating down the fiber, the laser light excited the SPR of the antenna array, generating a SERS signal from the self-assembled monolayer (SAM) of benzenethiol absorbed on the gold antennas. The objective lens collected both the Raman signal and light at the excitation wavelength that propagated back through the fiber. We removed the latter with a notch filter (Kaiser Optical Systems, Inc., Holographic NotchPlus Filter, center wavelength = 632.8 nm) and directed the remaining light into a Horiba Jobin Yvon Triax 550 spectrometer (entrance

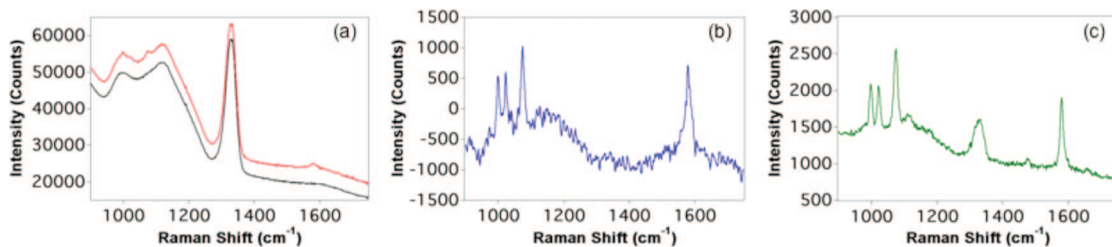


Figure 2. (a) Spectra recorded from a fiber optic probe featuring an array of SERS-active optical antennas integrated on the facet of the fiber (red, offset upward by 5000 counts) and a bare reference fiber (black), after both the transferred array and one facet of the bare fiber were immersed in a benzenethiol solution. (b) The difference of the SERS probe and reference fiber spectra. (c) SERS spectrum measured after placing the transferred array (coated with a monolayer of benzenethiol) in the focus of the objective lens.

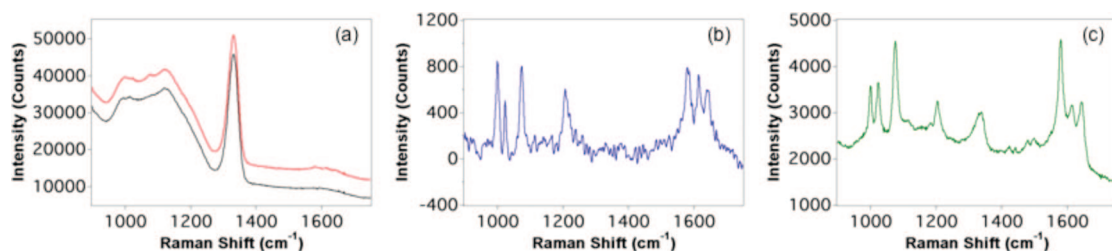


Figure 3. (a) Raman spectra recorded from a SERS probe (red, offset upward by 5000 counts) and a bare reference fiber (black) after soaking the fibers in a benzenethiol solution and subsequently submerging them in a 4-[(*E*)-2-pyridin-4-ylethenyl]pyridine solution. (b) Spectra obtained by subtracting the reference fiber spectrum from the SERS fiber probe spectrum. Raman peaks from both the benzenethiol (995, 1020, 1075, and 1583 cm^{-1}) and the 4-[(*E*)-2-pyridin-4-ylethenyl]pyridine (1207, 1616, and 1642 cm^{-1}) are apparent. (c) SERS spectrum measured after moving the transferred optical antennas into the focus of the objective lens and placing a drop of the 4-[(*E*)-2-pyridin-4-ylethenyl]pyridine solution onto the array.

slit = 200 μm). A holographic grating with groove density of 600 grooves/mm (Horiba Jobin Yvon) dispersed the light, and a thermoelectrically cooled silicon CCD camera collected the light.

The spectrum acquired from the SERS fiber probe (after soaking in the benzenethiol solution) is shown in red in Figure 2a, and the spectrum acquired from a bare, unmodified fiber of equal length is shown in black in Figure 2a; one facet of this reference fiber also soaked for 12 h in the benzenethiol solution but produced no measurable Raman signal. Both spectra were taken over a 40 s integration, with 5.4 mW of laser power focused on the fiber. Subtracting the reference fiber background from the SERS probe spectrum resulted in the “internal” illumination spectrum shown in Figure 2b. The Raman signal from four Raman-active vibrational modes of benzenethiol at 995, 1020, 1075, and 1583 cm^{-1} are readily apparent.²⁸ These peaks, which we acquired through the fiber, match the wavenumbers of the Raman peaks measured “externally” when we placed the modified facet of the probe in the focal plane of the objective lens, illuminated the array, and collected the resulting signal (Figure 2c, incident power = 0.46 mW, 10 s integration). This agreement indicates that the fiber does not artificially shift the peaks of the Raman signal. The broad feature at 1330 cm^{-1} originated from the silica fiber, not the benzenethiol, as demonstrated by the difference spectrum of Figure 2b.

When we measured the SERS spectra through the fiber optic probe, we did not observe a noticeable effect on the Raman signal when we used a half-wave plate to rotate the polarization of the laser light entering the objective lens or when we physically bent and twisted the fiber. We believe

the robustness of the measured signal results from the use of multimode nonpolarization maintaining fiber; light traveling through the fiber couples into different fiber modes before exciting the SPR of the array. The light in these modes spreads across the entire fiber core with polarization both parallel and perpendicular to the optical antennas. Thus, changing the polarization of input light (with the half-wave plate) or distributing light between different fiber modes (by bending the fiber) did not prevent excitation of the SPR of the array and affect the measured SERS signal.

To test the ability of the SERS probe to (i) detect multiple analytes simultaneously and (ii) perform measurements *in situ*, we submerged the facet of the SERS probe modified with benzenethiol and the facet of the reference fiber in a solution of 3 mM 4-[(*E*)-2-pyridin-4-ylethenyl]pyridine solution (“BPE”; Sigma Aldrich) in methanol and measured the spectra transmitted through the fibers. Figure 3a shows the spectrum measured from the probe (in red) and the spectrum of the bare reference fiber (in black). Both spectra represent a 40 s integration with 5.4 mW of power coupled into fiber. Figure 3b shows the spectrum obtained by subtracting the spectrum of the reference fiber from the spectrum of the SERS probe. The Raman signal from the benzenethiol is still apparent, and the BPE signals at 1207, 1616, and 1642 cm^{-1} are also visible.²⁹ We observed benzenethiol and BPE Raman peaks at these same wavenumbers when we positioned the array in the focus of the objective lens and covered the optical antennas with a drop of the BPE solution; this result illustrates that collecting signal through the fiber did not shift the position of the measured Raman peaks. The spectrum from this measurement is shown in Figure 3c (10 s integration, 0.7 mW power focused on the array). The feature

at 1330 cm^{-1} results from the silica fiber, rather than from the benzenethiol or BPE.

The strength of the Raman peak at 995 cm^{-1} in Figure 3b is increased relative to the other measured Raman peaks of benzenethiol. We believe this apparent increase occurs because this spectrum is not directly measured but is the difference between the probe and the reference fiber spectra. The magnitudes of the features in both of these measurements were affected by small changes in the coupling of light into the fibers. Independent alignments and measurements were carried out for these two spectra, resulting in nonzero differences between their backgrounds. These offsets are apparent in the uneven background of Figures 2b and 3b and are large enough to shift the relative heights of different Raman peaks. The use of a different fiber with a weaker background signal could allow direct use of the measured probe spectra and prevent these discrepancies.

The SERS signal from the BPE is still detectable, albeit with reduced intensity, when the fiber is removed from the BPE solution, rinsed gently with methanol, and dried. This decreased measurement from the dried fiber has two implications: (i) BPE molecules were absorbed on the gold antennas in areas where the benzenethiol SAM suffered from voids and packing disorder,^{30,31} and (ii) the signal from the submerged fiber came from both absorbed BPE molecules and the BPE molecules in the analyte solution. We detected Raman signals from both analytes after submerging probes (i) first into benzenethiol and then BPE (Figures 2 and 3), (ii) first into BPE and then benzenethiol (not shown), and (iii) a solution containing both benzenethiol and BPE (not shown).

The strong background features in the measurement from the SERS probe and the features in the spectra from the reference fiber are the same: both can be attributed to Raman scattering of the silica and GeO_2 and P_2O_5 dopants comprising the fiber core.³² Raman bands at $\sim 1000\text{--}1150\text{ cm}^{-1}$ have been shown to result from stretching vibrations of the mixed Si-O-Ge bonds and the Si-O bonds.³² The strong feature centered around 1330 cm^{-1} matches the position of the Raman band resulting from GeO_2 and P_2O_5 dopant incorporation into silica.³² This peak is evident in both the SERS probe and reference fiber measurements (Figures 2a and 3a) and the spectra taken directly from the optical antenna arrays (Figure 2c and 3c).

Enhancement Factor Calculations. The enhancement factor is the standard figure of merit used to compare the efficiencies of different SERS surfaces. The EF quantifies the ability of a SERS substrate to enhance the Raman signal of nearby analytes and is typically determined by comparing the Raman signal-per-molecule (i.e., the intensity of the Raman signal, I_{SERS} , normalized by the number of molecules contributing to the signal, N_{SERS}), to the Raman signal per molecule ($I_{\text{neat}}/N_{\text{neat}}$) generated by a non-SERS active reference (in this case, neat liquid benzenethiol). We calculated the average EF of the entire array of optical antennas, rather than the EF from a single localized hot spot. We used methods outlined by Cai et al.³³ to calculate the EF and only outline the calculation method here (the Supporting Informa-

tion contains EF calculation details). Equation 1 defines the EF.³⁴

$$\text{EF} = \left(\frac{I_{\text{SERS}}}{N_{\text{SERS}}} \right) \left(\frac{N_{\text{neat}}}{I_{\text{neat}}} \right) \quad (1)$$

We used the SERS spectra of the transferred array to determine the EF of the antennas. We collected Raman spectra of benzenethiol from the array using two different measurement configurations: “internal” (both the incident light and the Raman signal collected by the probe propagating through the fiber) and “external” (we focused the incident light directly on the transferred optical antennas and measured the SERS signal directly from the surface of the array). These spectra are shown in Figures 2b and 2c, respectively.

The external configuration is identical to the configuration typically used to collect SERS spectra for EF calculations.^{9,11,33} Using the SERS spectrum shown in Figure 2c, we determined values of I_{SERS} by measuring the heights of the benzenethiol Raman peaks relative to the nonzero baseline. The uniform size and periodic arrangement of the antennas enabled calculation of the number of benzenethiol molecules contributing to the signal (N_{SERS}). We recorded the corresponding reference measurement, which provided I_{neat} values, after placing a vial of liquid neat benzenethiol at the focal plane of the objective lens, and determined the number of molecules that contributed to this signal (N_{neat}).³³

We found EF values of 2.7×10^5 at 995 cm^{-1} , 2.6×10^5 at 1020 cm^{-1} , 5.1×10^5 at 1075 cm^{-1} , and 3.2×10^5 at 1583 cm^{-1} . This magnitude of EF is expected when the SERS calculations represent the average Raman enhancement across a SERS surface, rather than the EF of a single hot spot.^{9,34}

We sought to calculate the EF of the internal configuration (the spectrum shown in Figure 2b) since this is the configuration utilized for *in situ* detection. In principle, the EF values of the array undergoing internal and external illumination should be the same, since the EF is determined by the geometry of the optical antennas: similar internal and external EF values would indicate an efficient collection of SERS signal by the probe in the internal illumination experiment.

We expected some variation in the EF values to arise from the different collection efficiencies of the external and internal illumination configurations. In the two measurements we detected a different percentage of the total Raman scattering because (i) the numerical aperture (NA) of the objective lens and the fiber differed and (ii) only a portion of the SERS signal that propagated down the fiber during internal illumination was sent to the spectrometer.

With external illumination, the numerical aperture (NA) of the microscope objective (NA = 0.42) dictated that $\sim 4.6\%$ of the Raman signal from the benzenethiol (scattered over a solid angle of 2π) was collected by the objective lens and sent to the spectrometer. With internal illumination, the lower numerical aperture of the fiber (NA = 0.275) resulted in a smaller fraction ($\sim 1.9\%$) of the total SERS signal coupling into the fiber. Additionally, in the internal configuration we measured only a fraction of the SERS signal guided by the

fiber; the Raman signal enhanced by the optical antennas propagated along the entire core of the fiber (62.5 μm in diameter), but only a fraction ($\sim 2.5\%$) of the signal was collected by the objective lens ($\sim 10\ \mu\text{m}$ diameter spot size) and sent to the spectrometer.

To compensate for the reduced collection efficiency of the internal illumination measurement (compared to the external configuration) and obtain a detectable SERS signal (I_{SERS} values for eq 1), we increased the power of the light illuminating the array; we coupled 5.4 mW of power into the fiber during internal illumination (versus 0.46 mW during external illumination). Additionally, we used an integration time of 40 s to obtain the internal measurements (versus 10 s to obtain the external measurements). On the basis of these conditions, we obtained a value for the internal I_{SERS} from Figure 2b.

To complete the calculation of EF (eq 1) for the internal configuration, a reference Raman spectrum is needed to determine values of I_{neat} . To serve as a valid reference, this spectrum must be acquired with the same parameters (illumination power and integration time) used to generate the SERS spectrum in the internal configuration. We attempted to obtain I_{neat} values by collecting a Raman signal through an unmodified fiber with a bare facet submerged in neat benzenethiol. When we coupled 5.4 mW of illumination into the bare fiber and integrated for 40 s, no spectrum from the neat benzenethiol could be detected; this result illustrates the importance of the SERS array for *in situ* Raman signal detection.

Without the reference I_{neat} values, we could not use eq 1 to calculate the internal EF of the transferred array. Instead, we chose to approximate the internal EF by obtaining I_{neat} values from an alternate reference measurement: the Raman spectrum generated by a vial of neat benzenethiol placed directly in the focus of the objective lens. This is the same configuration used to measure the external EF reference spectrum. We attempted to obtain the alternate reference spectrum by illuminating the neat benzenethiol with the same measurement conditions used to determine I_{SERS} (40 s integration, 5.4 mW power), but these conditions saturated the CCD detector. We therefore focused light with a reduced intensity (0.46 mW, 40 s integration) into the neat benzenethiol to obtain a reference spectrum for the effective internal EF calculation.

To calculate an effective internal EF, we added a scaling factor to eq 1 to compensate for the differences between the SERS measurement obtained from the array with internal illumination and the external reference measurement of neat benzenethiol. We accounted for two differences: (i) the intensity of illumination and (ii) collection efficiency. Details of the scaling factor are found in the Supporting Information. To simplify the effective internal EF calculations, we assumed (i) a uniform distribution of unpolarized light across the core of the fiber, (ii) an equal SERS signal contribution from the optical antennas in the transferred array, and (iii) negligible optical absorption in the fiber.

We determined effective internal EF values of the array of 4.2×10^5 at $995\ \text{cm}^{-1}$, 5.1×10^5 at $1020\ \text{cm}^{-1}$, $6.4 \times$

10^5 at $1075\ \text{cm}^{-1}$, and 6.5×10^5 at $1583\ \text{cm}^{-1}$. These effective internal EF values are similar to the calculated external EF values, suggesting that an array of optical antennas can be effectively utilized as a Raman enhancing surface on a fiber optic probe for SERS detection; internal illumination does not compromise the detection of enhanced Raman signal of analytes near the antennas.

Conclusion. We demonstrated the ability of a fiber optic probe, comprising a lithographically defined array of coupled gold optical antennas transferred to the facet of an optical fiber, to simultaneously collect a SERS signal from multiple analytes. We chose the shape and spacing of the antennas to control the optical response of the probe and produce enhancement of the excitation light and the Raman signal of the analytes. We performed remote *in situ* chemical detection of multiple analytes with a single probe and utilized the periodicity of the array of optical antennas to determine the EF of the SERS surface, thereby providing a figure of merit to quantify the SERS probe performance. The transfer of lithographically defined patterns with higher EF values (e.g., nanoparticles with optimized shapes and/or separated by smaller gaps) could further enhance the SERS signal generated by the probe and result in the measurement of a stronger Raman signal. The use of an optical fiber with weaker background signal (due to different amounts and types of dopants) could eliminate the need to subtract the fiber background to observe the SERS signal of analytes and enable more optical power to be coupled into the probe. This change would allow for the detection of smaller concentrations of analytes, as well as the detection of weak Raman peaks of analytes that are hard to observe in the presence of a strong background signal from the fiber. This probe—a flexible fiber optic capable of SERS detection—can be used for many different applications, such as sensing samples in remote locations, probing samples with small volumes, and performing *in situ* measurements.

Acknowledgment. E.J.S. and F.C. are supported by the Defense Advanced Research Projects Agency under Award No. HR0011-06-1-0044. G.M.W. is supported by the California Institute of Technology Center for Optofluidic Integration supported by the Defense Advanced Research Projects Agency under award number HR0011-04-1-0032, and the National Institutes of Health under Contract NIEHS # ES016665. This work was performed in part at the Center for Nanoscale Systems (CNS) at Harvard University, a member of the National Nanotechnology Infrastructure Network (NNIN). The authors thank E. Diebold for valuable discussions.

Supporting Information Available: A figure showing SPR measured from arrays of optical antennas and additional details of the external and effective internal EF. This material is available free of charge via the Internet at <http://pubs.acs.org>.

References

- (1) Smythe, E. J.; Dickey, M. D.; Whitesides, G. M.; Capasso, F. A technique to transfer metallic nanoscale patterns to small and non-planar surfaces. *ACS Nano* **2009**, *3*, 59–65.
- (2) Novotny, L.; Hecht, B. *Principles of Nano-Optics*; Cambridge University Press: Cambridge, 2006.

- (3) Liu, Z.; Yang, Z. L.; Cui, L.; Ren, B.; Tian, Z. Q. Electrochemically roughened palladium electrodes for surface-enhanced Raman spectroscopy: Methodology, mechanism, and application. *J. Phys. Chem. C* **2007**, *111* (4), 1770–1775.
- (4) Yang, K. H.; Liu, Y. C.; Yu, C. C. Enhancements in intensity and stability of surface-enhanced Raman scattering on optimally electrochemically roughened silver substrates. *J. Mater. Chem.* **2008**, *18* (40), 4849–4855.
- (5) Fleischmann, M.; Hendra, P. J.; Mcquillan, A. Raman-spectra of pyridine adsorbed at a silver electrode. *Chem. Phys. Lett.* **1974**, *26* (2), 163–166.
- (6) Hayashi, S. SERS on random rough silver surfaces - evidence of surface-plasmon excitation and the enhancement factor for copper phthalocyanine. *Surf. Sci.* **1985**, *158* (1–3), 229–237.
- (7) Kneipp, K.; Kneipp, H.; Itzkan, I.; Dasari, R. R.; Feld, M. S. Surface-enhanced Raman scattering and biophysics. *J. Phys.: Condens. Matter* **2002**, *14* (18), R597–R624.
- (8) Grand, J.; de la Chapelle, M. L.; Bijeon, J. L.; Adam, P. M.; Vial, A.; Royer, P. Role of localized surface plasmons in surface-enhanced Raman scattering of shape-controlled metallic particles in regular arrays. *Phys. Rev. B* **2005**, *72* (3), 033407.
- (9) Laurent, G.; Felidj, N.; Aubard, J.; Levi, G.; Krenn, J. R.; Hohenau, A.; Schider, G.; Leitner, A.; Aussenegg, F. R. Evidence of multipolar excitations in surface enhanced Raman scattering. *Phys. Rev. B* **2005**, *71* (4), 045430.
- (10) McFarland, A. D.; Young, M. A.; Dieringer, J. A.; Van Duyne, R. P. Wavelength-scanned surface-enhanced Raman excitation spectroscopy. *J. Phys. Chem. B* **2005**, *109* (22), 11279–11285.
- (11) Felidj, N.; Aubard, J.; Levi, G.; Krenn, J. R.; Hohenau, A.; Schider, G.; Leitner, A.; Aussenegg, F. R. Optimized surface-enhanced Raman scattering on gold nanoparticle arrays. *Appl. Phys. Lett.* **2003**, *82* (18), 3095–3097.
- (12) Smythe, E. J.; Cubukcu, E.; Capasso, F. Optical properties of surface plasmon resonances of coupled metallic nanorods. *Opt. Express* **2007**, *15* (12), 7439–7447.
- (13) Bello, J. M.; Narayanan, V. A.; Stokes, D. L.; Vo-Dinh, T. Fiber optic remote sensor for in situ surface-enhanced Raman scattering analysis. *Anal. Chem.* **1990**, *62* (22), 2437–2441.
- (14) Stokes, D. L.; Chi, Z. H.; Vo-Dinh, T. Surface-enhanced-Raman-scattering-inducing nanoprobe for spectrochemical analysis. *Appl. Spectrosc.* **2004**, *58* (3), 292–298.
- (15) Gessner, R.; Rosch, P.; Petry, R.; Schmitt, M.; Strehle, M. A.; Kiefer, W.; Popp, J. The application of a SERS fiber probe for the investigation of sensitive biological samples. *Analyst* **2004**, *129* (12), 1193–1199.
- (16) Hankus, M. E.; Li, H. G.; Gibson, G. J.; Cullum, B. M. Surface-enhanced Raman scattering-based nanoprobe for high-resolution, non-scanning chemical imaging. *Anal. Chem.* **2006**, *78* (21), 7535–7546.
- (17) Mullen, K. I.; Carron, K. T. Surface-enhanced raman-spectroscopy with abrasively modified fiber optic probes. *Anal. Chem.* **1991**, *63* (19), 2196–2199.
- (18) Cox, F. M.; Argyros, A.; Large, M. C. J.; Kalluri, S. Surface enhanced Raman scattering in a hollow core microstructured optical fiber. *Opt. Express* **2007**, *15* (21), 13675–13681.
- (19) Yan, H.; Gua, C.; Yang, C. X.; Liu, J.; Jin, G. F.; Zhang, J. T.; Hou, L. T.; Yao, Y. Hollow core photonic crystal fiber surface-enhanced Raman probe. *Appl. Phys. Lett.* **2006**, *89* (20), 204101.
- (20) Zhang, Y.; Shi, C.; Gu, C.; Seballos, L.; Zhang, J. Z. Liquid core photonic crystal fiber sensor based on surface enhanced Raman scattering. *Appl. Phys. Lett.* **2007**, *90* (19), 193504.
- (21) Viets, C.; Hill, W. Comparison of fibre-optic SERS sensors with differently prepared tips. *Sens. Actuators, B* **1998**, *51*, 92–99.
- (22) Viets, C.; Hill, W. Single-fibre surface-enhanced Raman sensors with angled tips. *J. Raman Spectrosc.* **2000**, *31* (7), 625–631.
- (23) Stokes, D. L.; Vo-Dinh, T. Development of an integrated single-fiber SERS sensor. *Sens. Actuators B* **2000**, *69* (1–2), 28–36.
- (24) Hulsteen, J. C.; Van Duyne, R. P. Nanosphere lithography - a materials general fabrication process for periodic particle array surfaces. *J. Vac. Sci. Technol., A* **1995**, *13* (3), 1553–1558.
- (25) Fu, Y. Q.; Bryan, N. K. A. Investigation of physical properties of quartz after focused ion beam bombardment. *Appl. Phys. B: Lasers Opt.* **2005**, *80* (4–5), 581–585.
- (26) Gunnarsson, L.; Rindzevicius, T.; Prikulis, J.; Kasemo, B.; Kall, M.; Zou, S. L.; Schatz, G. C. Confined plasmons in nanofabricated single silver particle pairs: Experimental observations of strong interparticle interactions. *J. Phys. Chem. B* **2005**, *109* (3), 1079–1087.
- (27) Kelly, K. L.; Coronado, E.; Zhao, L. L.; Schatz, G. C. The optical properties of metal nanoparticles: The influence of size, shape, and dielectric environment. *J. Phys. Chem. B* **2003**, *107* (3), 668–677.
- (28) Varsanyi, G. K.; M., A.; Lang, L. *Assignments for Vibrational Spectra of 700 Benzene Derivatives*; John Wiley & Sons: New York, 1974.
- (29) McMahon, J. J.; Babcock, G. T. Polycrystalline and solution raman-spectra of trans-1,2-Bis(4-Pyridyl)Ethylene, its dihydrochloride and its dideuteriochloride. *Spectrochim. Acta, Part A* **1982**, *38* (11), 1115–1122.
- (30) Van Duyne, R. P.; Hulsteen, J. C.; Treichel, D. A. Atomic-force microscopy and surface-enhanced raman-spectroscopy 0.1. Ag island films and Ag film over polymer nanosphere surfaces supported on glass. *J. Chem. Phys.* **1993**, *99* (3), 2101–2115.
- (31) Dhirani, A. A.; Zehner, R. W.; Hsung, R. P.; Guyot-Sionnest, P.; Sita, L. R. Self-assembly of conjugated molecular rods: A high-resolution STM study. *J. Am. Chem. Soc.* **1996**, *118* (13), 3319–3320.
- (32) Lan, G. L.; Banerjee, P. K.; Mitra, S. S. Raman-scattering in optical fibers. *J. Raman Spectrosc.* **1981**, *11* (5), 416–423.
- (33) Cai, W. B.; Ren, B.; Li, X. Q.; She, C. X.; Liu, F. M.; Cai, X. W.; Tian, Z. Q. Investigation of surface-enhanced Raman scattering from platinum electrodes using a confocal Raman microscope: dependence of surface roughening pretreatment. *Surf. Sci.* **1998**, *406* (1–3), 9–22.
- (34) Le Ru, E. C.; Blackie, E.; Meyer, M.; Etchegoin, P. G. Surface enhanced Raman scattering enhancement factors: a comprehensive study. *J. Phys. Chem. C* **2007**, *111* (37), 13794–13803.

NL803668U